Journal of Power Sources 196 (2011) 5377–5385

Contents lists available at ScienceDirect

Journal of Power Sources

journal homepage: www.elsevier.com/locate/jpowsour

A visualization study on relationship between water-droplet behavior and cell voltage appeared in straight, parallel and serpentine channel pattern cells

Hiromitsu Masuda, Atsushi Yamamoto, Kazunari Sasaki, Sangkun Lee, Kohei Ito*

Graduate School of Engineering, Kyushu University, Japan

ARTICLE INFO

Article history:
Received 17 November 2010
Received in revised form 18 February 2011
Accepted 22 February 2011
Available online 26 February 2011

Keywords:
Channel pattern
Water droplet
Flooding
Plugging and flushing

ABSTRACT

It is a critical issue to understand the relationship between water-droplet behavior and cell voltage for the establishment of PEFC water management. We fabricated three cells, whose channel pattern is different: straight one channel, parallel three channels and serpentine one channel. We operated these different channel-pattern cells and visualized water droplets in cathode channel, with systematically changing operation condition to quantitatively compare the performance and water droplet behavior between the cells. Successive process of water behavior, named as flooding, plugging and flushing, emerged in every channel-pattern cell. However, the each channel pattern cell also has inherent water behavior, showing particular cell voltage variation. Within our experimental condition, the serpentine one channel cell showed a superior tolerance to flooding and the highest performance among the three cells.

1. Introduction

Visualization cells have widely utilized to grasp the relationship between performance and water behavior in PEFC. The visualization cell has the separator where transparency material is built into, and it enable us to observe the water droplets in channel leading to understanding the impact of water droplet on cell performance. In addition to the water behavior in channel, new visualization techniques such as neutron imaging enable us to observe the water behavior in GDL and polymer electrolyte membrane in detail. Visualization study on PEFC recently orients to these high-technology-based methods. However, the visualization cell method seems to be still effective in PEFC R&D. This is because the visualization cell can observe the water droplet with rather simple experimental setup, and because it can estimate the water content in PEM and the saturation ratio in CL and GDL accompanying with impedance analysis.

Many visualization studies on water behavior in PEFC have been done both with visualization cells and neutron imaging as mentioned. Tüber et al. showed the impact of the water droplet in channel on the cell voltage with visualization cell, and showed the threshold of gas utilization ratio when flooding in the channel emerges [1]. Zhang et al. investigated with a visualization cell, which had the parallel seven channels, and gave the relationship between water behavior and gas velocity in channel, and indicated the specific conditions when water droplet removed from channel [2]. Liu et al. fabricated and operated an interdigitated and cascade channel cell with visualization window. Their cells showed small amount of water accumulation in channel and indicated less impact of flooding on cell voltage comparing with conventional cells such as parallel pattern cell [3]. Moreover, they mentioned that lower cell-temperature promoted lager flooding in cathode channel [4]. Turhan and Kowal et al. visualized several cells under various operation condition, and showed characteristic water-behaviors for each cell. Parallel pattern channel cell showed that increasing the flow rate in the channel enhanced the drainage of the water in GDL under channel, although the enhancement was not effective for the water in GDL under rib [5,6]. Serpentine pattern channel accumulated water especially near the corner of the channel, and then the water plugged the channel and was flushed. This successive water process appeared at several minute interval, resulting in periodic change of cell voltage [7].

Thus the visualization studies contributed to give a certain understanding on the relationship between water behavior and cell performance. However, it seems that their study, used rather complex and large cell, could not reach a quantitative understanding of the channel pattern impact on water behavior with systematically manner. We still wonder if each channel pattern cell has its intrinsic relationship between water behavior and cell output. This situation, where the information of the relationship is being lacked, blocks to optimize channel pattern for flooding tolerance.

To figure out the impact of channel pattern on water behavior, we executed a visualization study with the basic cells, whose channel-pattern on each was different and step-wisely complex

* Corresponding author at: Kyushu University, Faculty of Engineering, Department of Mechanical Engineering and Science, Motooka 744, Nishi-ku, Fukuoka-shi, Fukuoka 819-0395, Japan. Tel.: +81 92 802 3144; fax: +81 92 802 0001.
E-mail address: kohei@mech.kyushu-u.ac.jp (K. Ito).

0378-7753/$ – see front matter © 2011 Elsevier B.V. All rights reserved.
doi:10.1016/j.jpowsour.2011.02.074

Table 1
Cell dimension.

Description (axis)	Dimension Straight one channel cell	Parallel three channels cell	Serpentine one channel cell
Length of GFC (x)	30 mm	30 mm	94 mm
Width of GFC (y)	1.6 mm	1.0 mm	1.0 mm
Height of GFC (z)	1.0 mm	1.0 mm	1.0 mm
Cross section of GFC (yz)	1.6 mm^2	3 mm^2	1 mm^2
Width of land (y)	1.6 mm	1.0 mm	1.0 mm
Length of GDL (x)	31.5 mm	31.5 mm	31.5 mm
Width of GDL (y)	3.2 mm	6 mm	6 mm
Thickness of GDL (z)	400 μm	400 μm	400 μm
Active area (xy)	1.0 cm^2	1.9 cm^2	1.9 cm^2

design: straight one channel, parallel three channels and serpentine one channel. We operated and visualized these different channel-pattern cells systematically adjusting operation condition so that current density, gas utilization ratio, or the gas velocity at cathode channel inlet was same between the cells. The different channel-pattern cell showed the different cell voltage variation, which could be explained by the visualized water behavior as shown in the followings.

2. Experimental

The visualization cell, which has different channel pattern shown in Fig. 1, was designed and fabricated to investigate the relationship between cell performance and water behavior. Straight one channel cell is expected to grasp an essential behavior of liquid water in channel: water droplet starts to accumulate at downstream, and its accumulation causes, so-called, plugging and flushing in the channel, leading to stopping electricity generation at worse. Comparing the straight one channel cell, the parallel three channel cell shown in the Figure is expected to understand its inherent feature such as inter-channel coordination when a channel is plugged by water droplet. The serpentine one channel listed has longer channel path than others, resulting in a frequent water-accumulation especially at downstream. However, this channel pattern can give a gas flow under rib to help the drainage of water in GDL [8]. Thus the serpentine one channel is expected to evaluate this trade-off effect.

The dimensions of each channel are listed in Table 1. The length of the serpentine one channel is three times lager than that of the straight one channel. Effective electrode area is assumed to be equal to the area where GDL contacts with MEA. With this assumption, the effective electrode area of parallel three channels and serpentine one channel is twice comparing to that of straight one channel. These dimensions, carefully considered, enables us to methodically compare the performance between different channel-pattern cells as shown in the Section 3.

Every channel-pattern cell embodies a commercial MEA, which is sandwiched with the two piece of carbon cloth GDL and the two piece of separator made of SUS 316 with gold plating. These were assembled with tightening bolts and nuts so that compression was 1 MPa. Each channel-pattern cell was placed in thermostatic chamber to control cell temperature. Cathode channel was observed with a microscope (KEYENCE VX-200) through chamber window. AC impedance spectroscopy was done to grasp Ohmic resistance and non-Ohmic resistance during cell operation. The non-Ohmic resistance was estimated as to be the length between the two intercepts crossing real axis at high and low frequency on cole-cole diagram from the AC impedance spectroscopy. Capturing image and measuring the resistances were done in every several minutes.

Table 2
Operation conditions: oxygen utilization ratio with methodologically changing current density and air flow rate.

Straight one channel cell		Air flow rate (sccm)/Air velocity (m s^{-1}) 58/0.60	116/1.21	232/2.42
Current density [A cm^{-2}]	0.15	0.05	0.025	0.0125
	0.30	0.1	0.05	0.025
	0.60	0.2	0.1	0.05

Straight three channels cell		Air flow rate (sccm)/Air velocity (m s^{-1}) 116/0.64	232/1.29	464/2.58
Current density [A cm^{-2}]	0.16	0.05	0.025	0.0125
	0.32	0.1	0.05	0.025
	0.63	0.2	0.1	0.05

Serpentine one channel cell		Air flow rate (sccm)/Air velocity (m s^{-1}) 78/1.28	116/1.93	232/3.87	464/7.73
Current density [A cm^{-2}]	0.16	0.075	0.05	0.025	0.0125
	0.32	0.15	0.1	0.05	0.025
	0.63	0.3	0.2	0.1	0.05

Table 2 shows the oxygen utilization ratio in cathode for the each channel-pattern cell. The oxygen utilization ratio was adjusted to be the range from 0.0125 to 0.3 by changing average current density and air flow rate (inlet flow velocity) simultaneously, as shown in the table. This methodical way to change the operation parameter leads to a reasonable comparison between different channel-pattern cells under the same condition of the oxygen utilization, current density or flow rate. The cell temperature of 30 °C and the relative humidity of 75%, which are categorized as a flooding condition, were chosen to observe the impact of water droplets on cell performance obviously. Hydrogen gas was supplied to anode, with the same utilization ratio in the case of cathode.

Before the each cell operation, a preliminary operation was conducted in the following. First, cell temperature, gas flow rate and relative humidity were adjusted as a specified condition in Table 2. Second, cell voltage was checked if it shows a reasonable open cell voltage without loading current. Third, the cell was idled under a low current density condition in 30 min. Just after this procedure, we started to operate the cell with a specified current density shown in Table 2, and visualized cathode channel with recording the time evolution of cell voltage and resistances.

3. Result and discussion

Relationship between water behavior and cell voltage is here evaluated for each channel-pattern cell. To give a consistency in the evaluation, it was done under the same operation condition of current density, oxygen utilization or air velocity at channel inlet.

3.1. Comparison under the same load-current density condition of 0.6 A cm^{-2}

The upper column in Fig. 2 indicates cell voltages for the different channel-pattern cells. The lower one indicates overvoltage resistance obtained from AC impedance spectroscopy. It is noted that IR resistance was relatively smaller than the overvoltage resistance, and was constant because a humidified condition was chosen as mentioned in the previous section. The three trends in the each diagram are corresponding to the different oxygen utilization ratio of 0.05, 0.1 and 0.2.

Every channel pattern cell showed the conventional characteristics where higher flow rate (lower utilization ratio) invited higher cell voltage and lower overvoltage resistance. This is because the

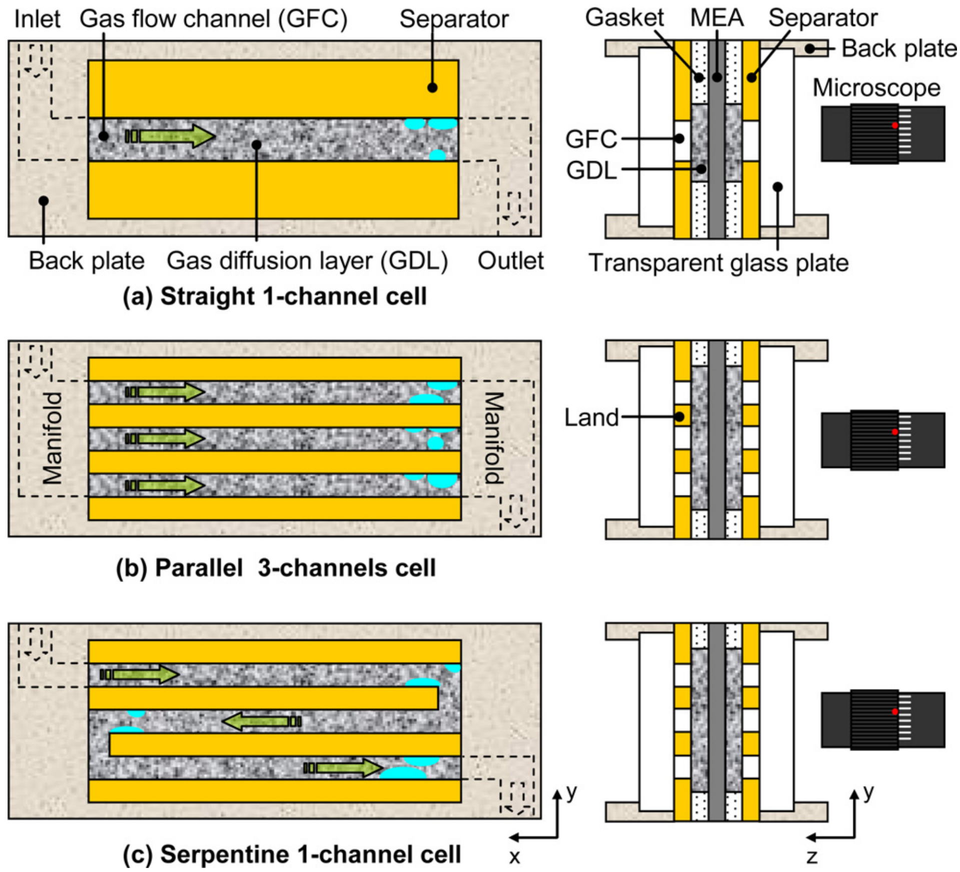

Fig. 1. Schema of visualization cell. (a) Straight one channel. (b) Parallel three channels. (c) Serpentine one channel.

higher flow rate promoted the drainage of water in channel and the effective gas-supply to CL. Among the three channel-pattern cells, the serpentine one channel cell had the highest stability and cell voltage. The parallel three channels cell and straight one channel cell had second and third performance, respectively. Generally, serpentine channel pattern cell can give convection flow under rib (land), which enhance the drainage of liquid water in GDL [8]. This unique characteristic of serpentine channel cell is thought to cause its high performance shown here.

The cell voltage in the case of the straight one channel cell showed two distinctive time-evolutions, which are monotonous decrease and sudden change in the following manner. The liquid water accumulated in GDL and channel as time elapsed disturbs oxygen supply to CL, leading to the monotonous decrease of cell voltage. The liquid accumulation reaches the maximum that the cell can storage liquid water, resulting in flushing with a sudden change of cell voltage. The sudden change of cell voltage develops into the following two cases: (i) sudden large decrease results in stopping electricity generation: (ii) sudden decrease turns to recover cell voltage. In the case of (i), the liquid water accumulated in channel causes a plugging in the channel; the plugging triggers off a flushing that flush liquid water in cell; the flushing forms water film on GDL surface; then it considerably blocks oxygen supply to CL, leading to stopping the power generation [9]. In the case of (ii) where cell voltage recovers, the flushing functions a priming to drain water in both GDL and channel, and turns the oxygen supply to adequate level.

These cell voltage evolutions of the monotonous decrease and sudden change, which were seen in the straight one channel, also appeared in the other cells of the parallel three channels and serpentine one channel. However the other cells have an adjacent channel, which leads to a different time and space characteristics of water accumulation and drainage, and superpose a particular cell voltage variation as shown in the following.

Comparing with the straight one channel cell (Fig. 2a), the cell voltage in the case of the parallel three channels cell (Fig. 2b) was rather stabilized. The monotonous decrease of the cell voltage was relatively slow, and the sudden change occasionally happened was small. It is worth to mention that the parallel three channels cell indicated a step-wise decrease in cell voltage under the condition of air flow rate 464 sccm in Fig. 2b. This feature observed only in the case of the parallel three channels cell.

Fig. 3 is the visualized image of the parallel three channels, taken at the specified time shown in Fig. 2b. Fig. 3a shows the channels just after the cell voltage decreased step-wisely. A plugging was observed near the inlet in a channel. As time elapsed, the plugging in the channel spread from the inlet to the outlet. Generally, plugging invites insufficient supply of oxygen gas to CL, resulting in a decrease of cell voltage. However, re-distribution of air supply to the other channels through the manifold placed at channel inlet permits continuous power generation to some extent. Thus, the parallel three channels cell did not reach the state of stopping power generation after plugging happens, and showed the step-wise cell voltage change that could not be seen in the case of the straight one channel cell.

Fig. 3c and d are the visualized images of the parallel three channels cell under the condition that air flow rate was relatively small. They show a larger amount of water droplets and a wider region of plugging. This is because smaller flow rate suppressed the drainage of droplets. With the cell voltage variation in the small flow rate condition shown in Fig. 2b, it is understood that smaller flow rate degrades the drainage of water, leading

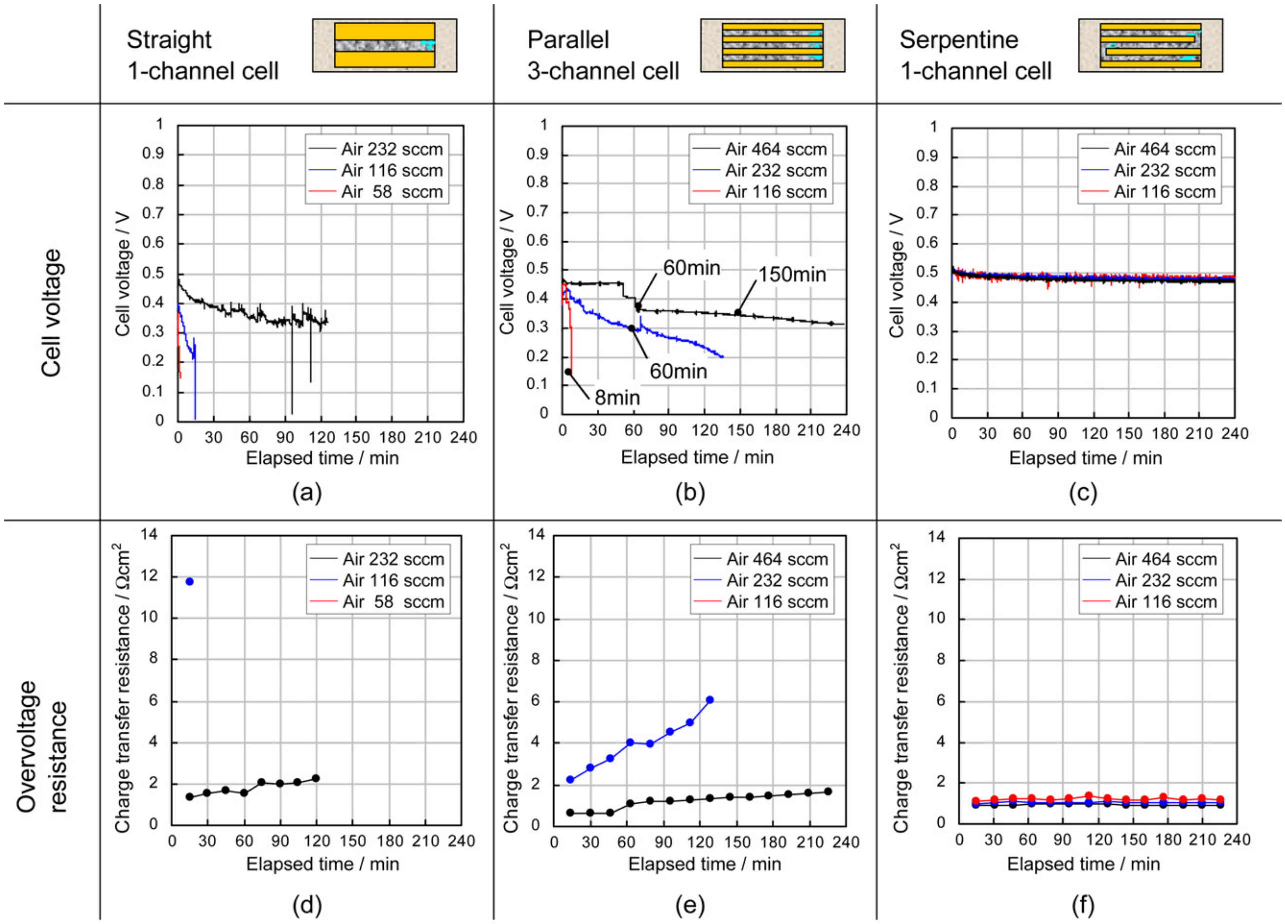

Fig. 2. Time variation of cell voltage and overvoltage resistance of the different channel-pattern cells under the same load-current condition of 0.6 A cm^{-2}.

to the larger water-accumulation in channel and lower cell voltage.

The performance in the case of the serpentine one channel cell was so superior that the cell could stably generate electricity during whole operation period as shown in Fig. 2c. Generally, serpentine cell gives a differential pressure between adjacent channels, and this differential pressure causes convection flow in GDL under rib, leading to the promotion for water drainage in GDL [8]. This mechanism is thought to have functioned in our serpentine one channel cell, resulting in the stable cell voltage. This discussion is also supported by Fig. 2f, where the overvoltage corresponding to water accumulation in our experimental condition was small.

A careful observation of the cell voltage measured from the serpentine one channel cell revealed a unique feature as shown in Fig. 4 that magnified Fig. 2c. The cell voltage changed like saw edge. The cell voltage periodically repeated a monotonous decrease and a sudden increase. The channel of the serpentine one channel cell has 3 times longer than that of other channel cell, resulting that the high vapor-pressure region spreads downstream. In addition the serpentine one channel cell forms flow stagnation at the corner in the channel, which becomes a trigger for forming water droplet. These two features are though to cause the periodic cell voltage change in the following mechanism. Water starts to certainly accumulate at the corner accompanying with the monotonous decrease of cell voltage. Then, the accumulated water leads to plugging the channel, and to flushing, which drainages the water both in the channel and GDL. The state in the cell goes back to the first stage with recovering cell voltage. Thus the cell voltage in the serpentine one channel cell showed the periodic cell voltage change like saw edge.

The other cells, whose channel pattern is different from serpentine channel, also experienced the successive process. However, the serpentine one channel cell can experience it with high repetition. In addition to the superior characteristics of drainage for the water in GDL by convection flow as mentioned above, this high repetition of the successive process of water accumulation, plugging, flushing and drainage is thought to stabilize the cell voltage of the serpentine one channel cell even when a flooding condition is imposed.

Fig. 5 is the visualized images of the serpentine one channel cell. Different images correspond to the different cases of flow rate, but were taken at a same elapsed time. As touched above, accumulated water was observed near the corner in channel, especially at downstream region. Moreover, these images suggest that slower flow rate enhanced the accumulation of water in channel. This suggestion links to a prediction that slower flow rate will give more frequent water-flushing and voltage-change. According to the prediction, the slower flow rate did give a more frequent voltage-change as shown in Fig. 4.

Fig. 6 is the summary, by schema, of the relationship between water behavior and cell voltage change for each channel pattern cell. The straight one channel cell slowly accumulates water leading to gradual flooding and plugging, and then experiences flushing immediately after the plugging formed in the channel. If, at that time, water film triggered by the flushing is formed on the surface of GDL, generating electricity stops as shown in Fig. 6(1). When the flushing drainages water in the channel and GDL with pump-priming effect, cell voltage recovers shown in Fig. 6(2). The parallel three channels cell also causes a gradual flooding and plugging. However, the following dissimilar processes progress: supplying

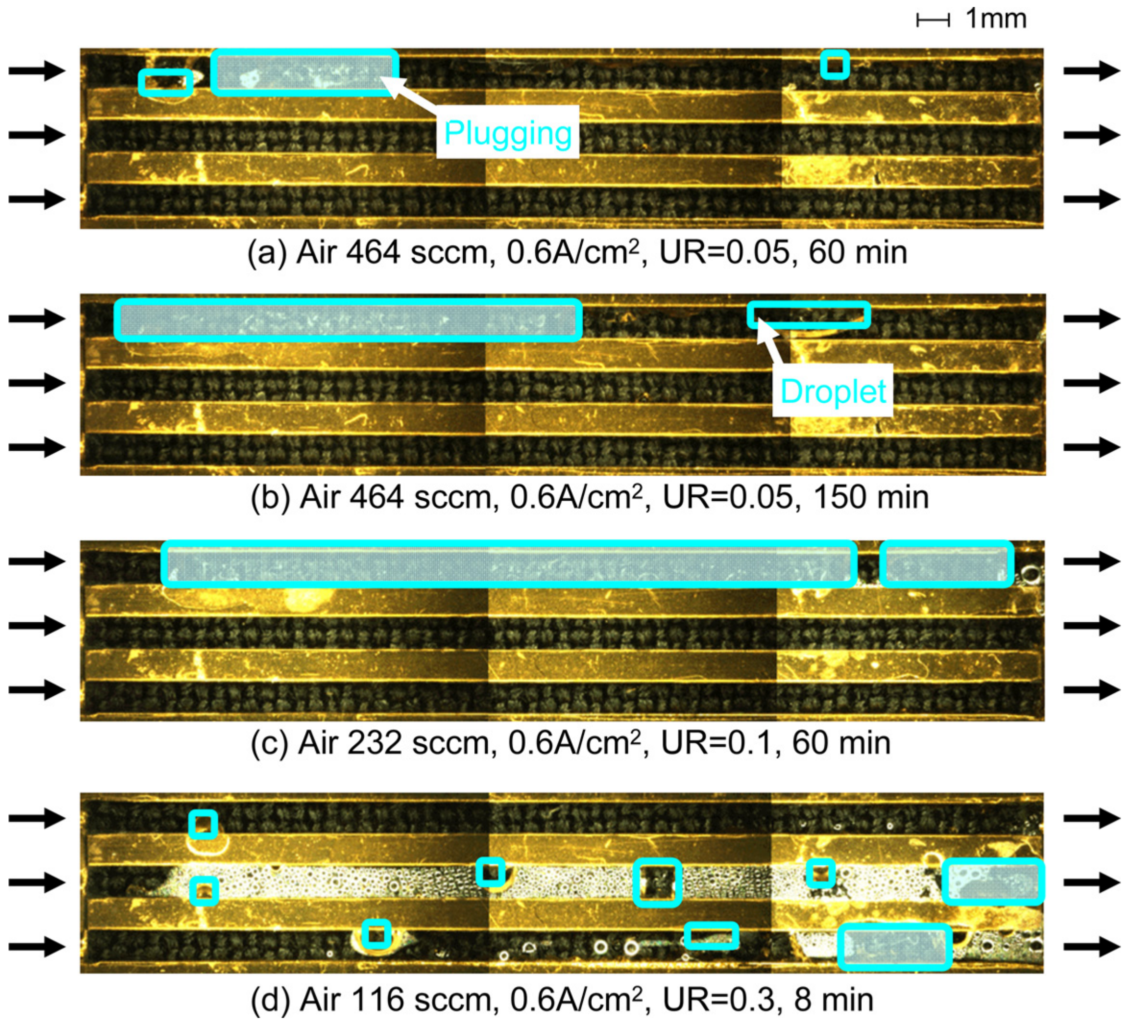

Fig. 3. Visualized images of the parallel three channel cell at the specified time under the same load-current of 0.6 A cm^{-2}. UR means oxygen utilization ratio.

gas is re-distributed through the manifold at channel inlet, and it helps generating electricity to continue, accompanying with a step-wise decrease of cell voltage as shown in Fig. 6(3): a flushing happened occasionally, and it allows cell voltage to recover shown in Fig. 6(4). The serpentine one channel cell causes a flooding especially near the corner in channel, leading to a plugging, flushing, water drainage and recovering cell voltage, and experiences this successive process frequently shown in Fig. 6(5).

3.2. Comparison under the same oxygen gas utilization condition of 0.05

Fig. 7 is cell voltage and overvoltage resistance of the different channel-pattern cells under the same oxygen gas utilization condition of 0.05, with the various load currents of 0.15, 0.3 and 0.6 A cm^{-2}. The tendency of cell voltage variation of the each different channel-pattern cell is similar to Fig. 2 that was the experiment result under a same current density condition of 0.6 A cm^{-2}. The cell voltage in the case of straight one channel cell indicated monotonous decrease and sudden change. That in the case of parallel three channels cell indicated step-wise change. That in the case of serpentine one channel cell indicated the change such as saw edge, although the change is rather difficult to see directly from Fig. 7.

In addition to these features that were also mentioned in Section 3.1, new information can be obtained from the comparison under the same oxygen utilization condition. The cell voltage of every channel-pattern cell was relatively unstable when the current density was adjusted to be the middle level of 0.3 A cm^{-2}. Indeed, the middle current density condition caused the shortest duration of generating electricity in the case of straight one channel cell. Also,

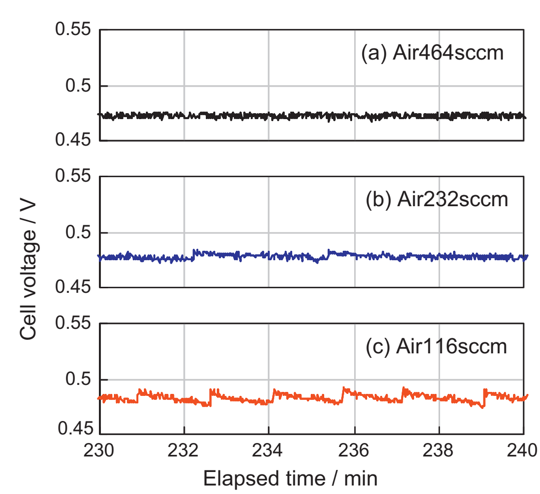

Fig. 4. Time variation of the cell voltage of the serpentine one channel. This is the enlarged-view from Fig. 2(c).

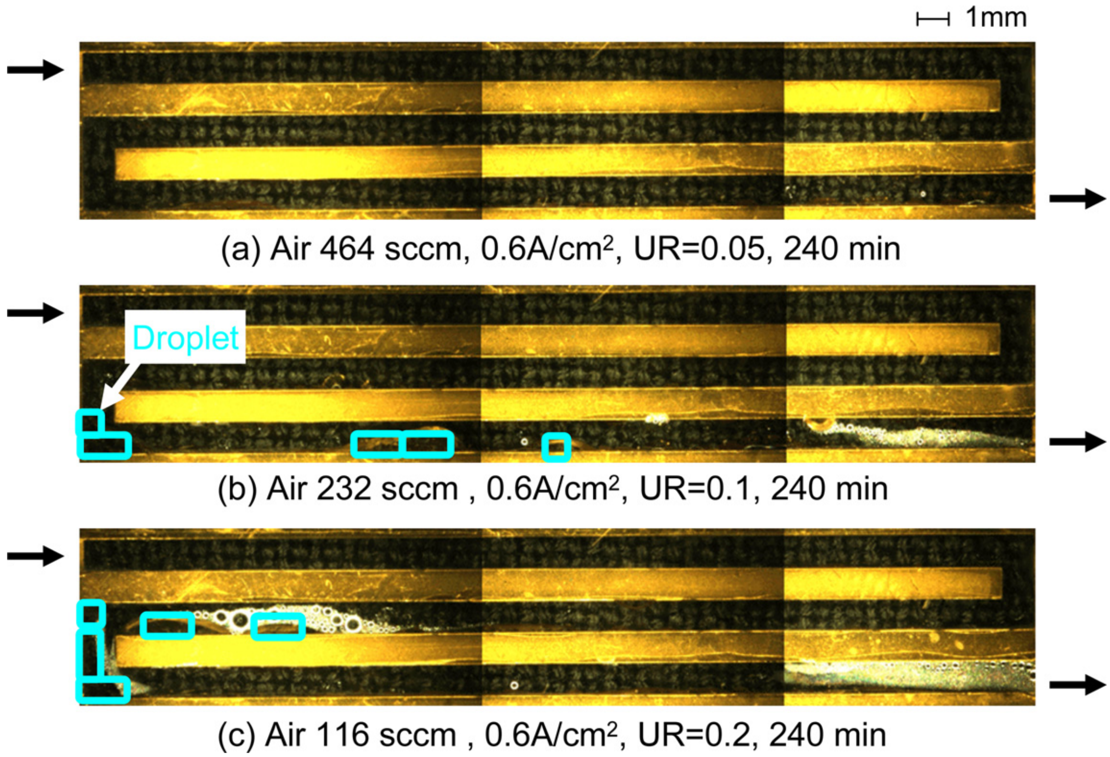

Fig. 5. Visualized images of the serpentine one channel cell at the specified time under the same load-current of 0.6 A cm^{-2}.

the middle current density condition triggered a large step-wise change of cell voltage in the case of parallel three channels cell.

The visualized image of channel can give a possible explanation for this interesting feature that the middle current density yielded unstable cell voltage although the oxygen utilization ratio was controlled to be same for any current density conditions. Fig. 8 is the visualized images in the case of straight one channel cell. The image a, b and c in the figure were respectively taken at 60 min elapsed under 0.15 A cm^{-2}, at 30 min under 0.3 A cm^{-2} and at 15 min under 0.6 A cm^{-2}, for aiming a specific comparison with a same amount of produced water which can be predicted by calculating the product of the elapsed time and current. From Fig. 8, it is observed that

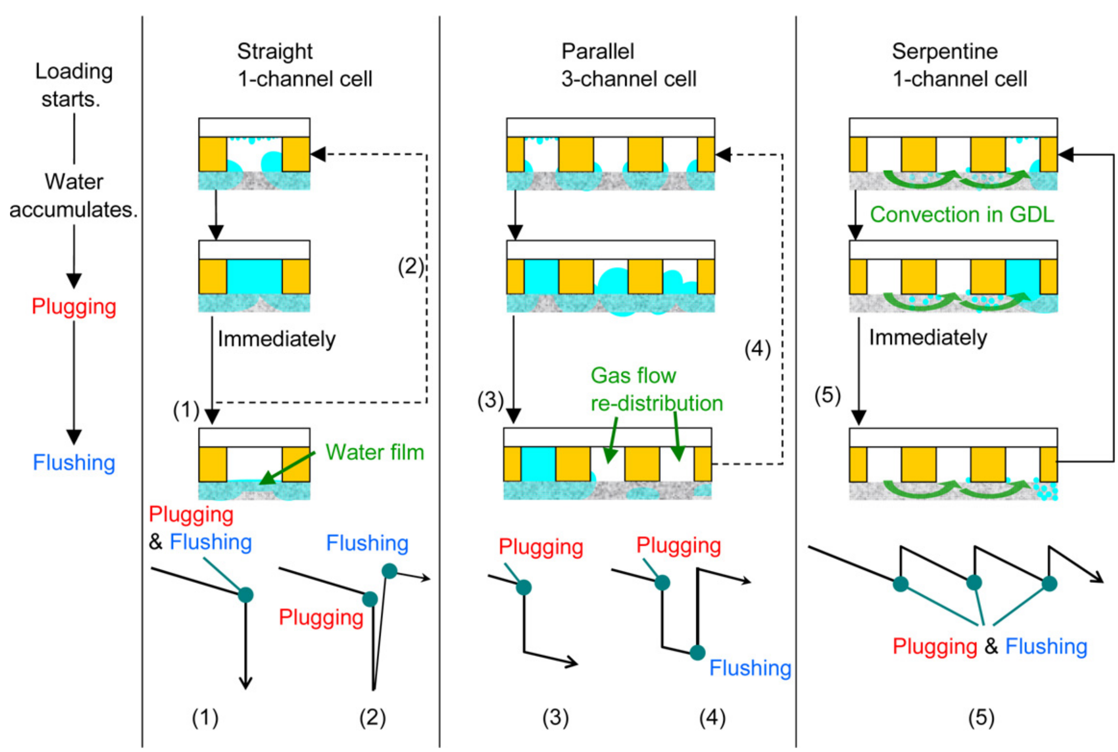

Fig. 6. Schema of the time evolution of water and cell voltage for the different channel pattern cells.

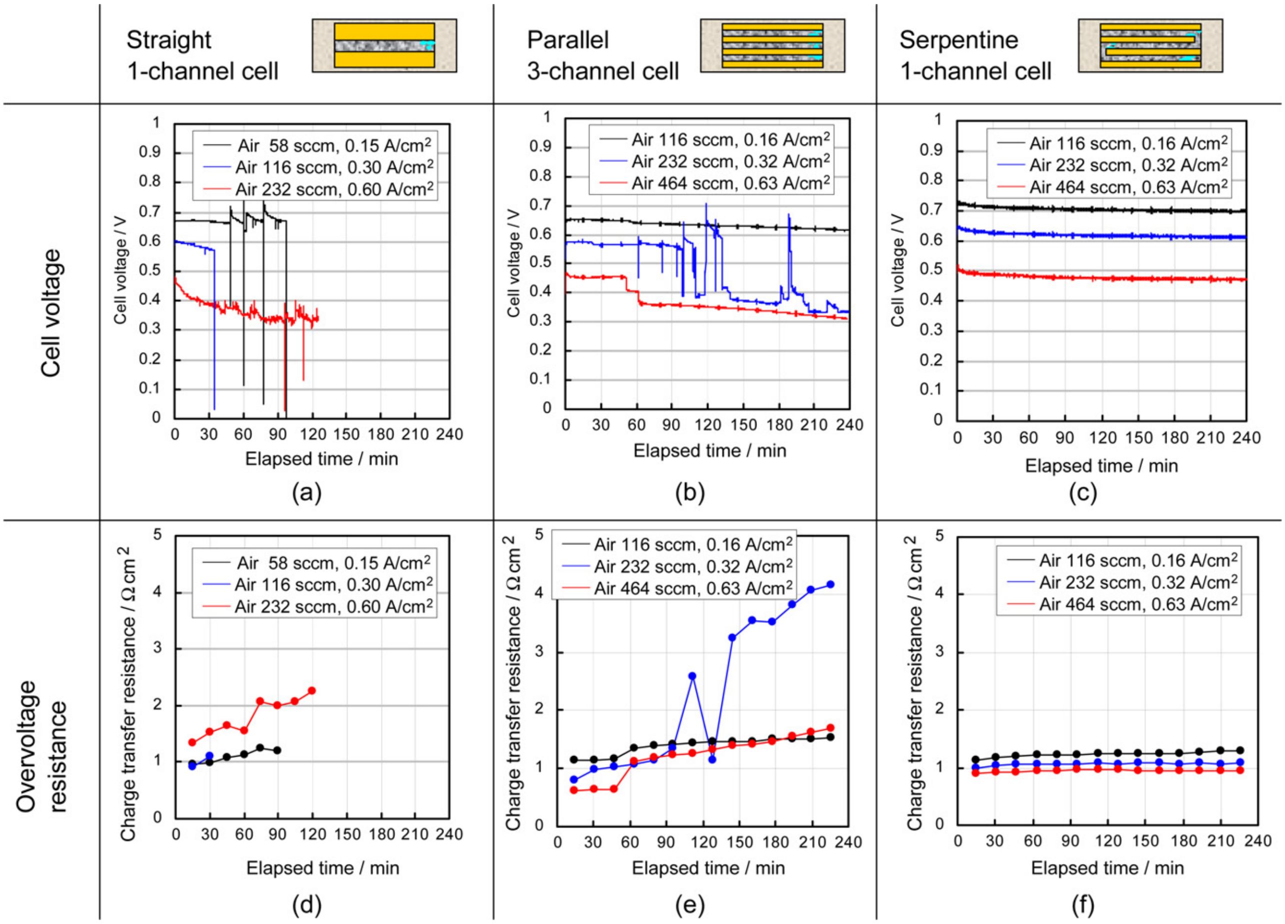

Fig. 7. Time variation of cell voltage and overvoltage resistance of the different channel pattern cells under the same oxygen utilization ratio condition of 0.05.

water was accumulated mostly in 0.3 A cm^{-2} condition, secondly in the 0.15 A cm^{-2}, thirdly in the 0.6 A cm^{-2} condition. Same feature appeared in the case of parallel three channels cell as shown in Fig. 9. Maximum water accumulation was shown under the middle level current density condition of ca. 0.3 A cm^{-2}. Thus, the most water-accumulation appeared in the middle level current density condition is thought to be the reason why the cell voltage, shown in Fig. 7a and b, was most unstable in this condition, although the constant oxygen utilization ratio of 0.05 was imposed in every cell operations.

Why did the middle current density condition, in the cases of the straight one channel and the parallel three channels cells, yield the maximum water-accumulation? Possible answer for this question can be given with considering the balance between water production and its drainage. The rate of water production R_{pro} is proportional to load current. On the other hand, the rate of water

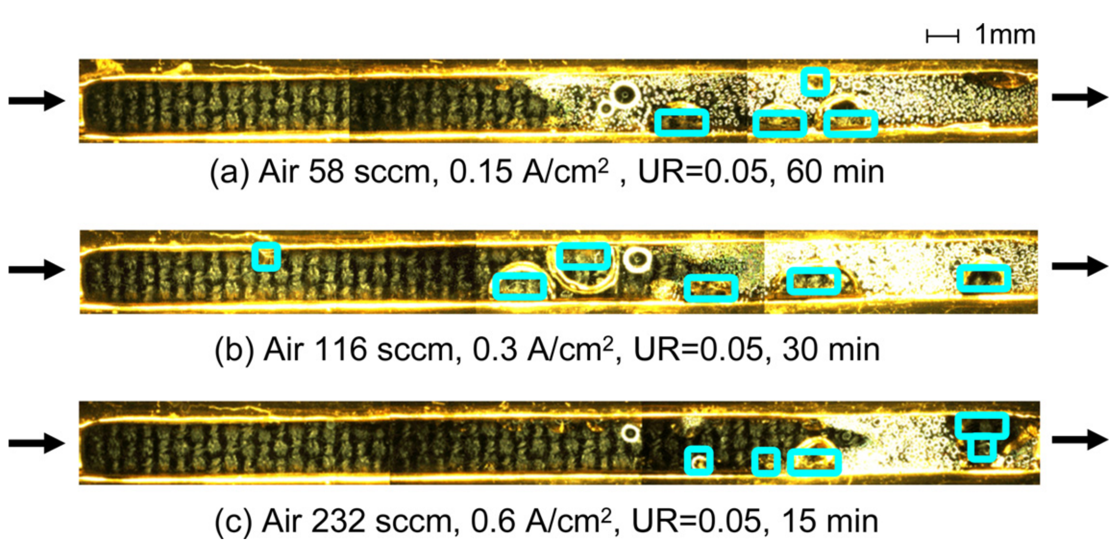

Fig. 8. Visualized images of the straight one channel cell at the specified time under the same oxygen utilization ratio condition of 0.05.

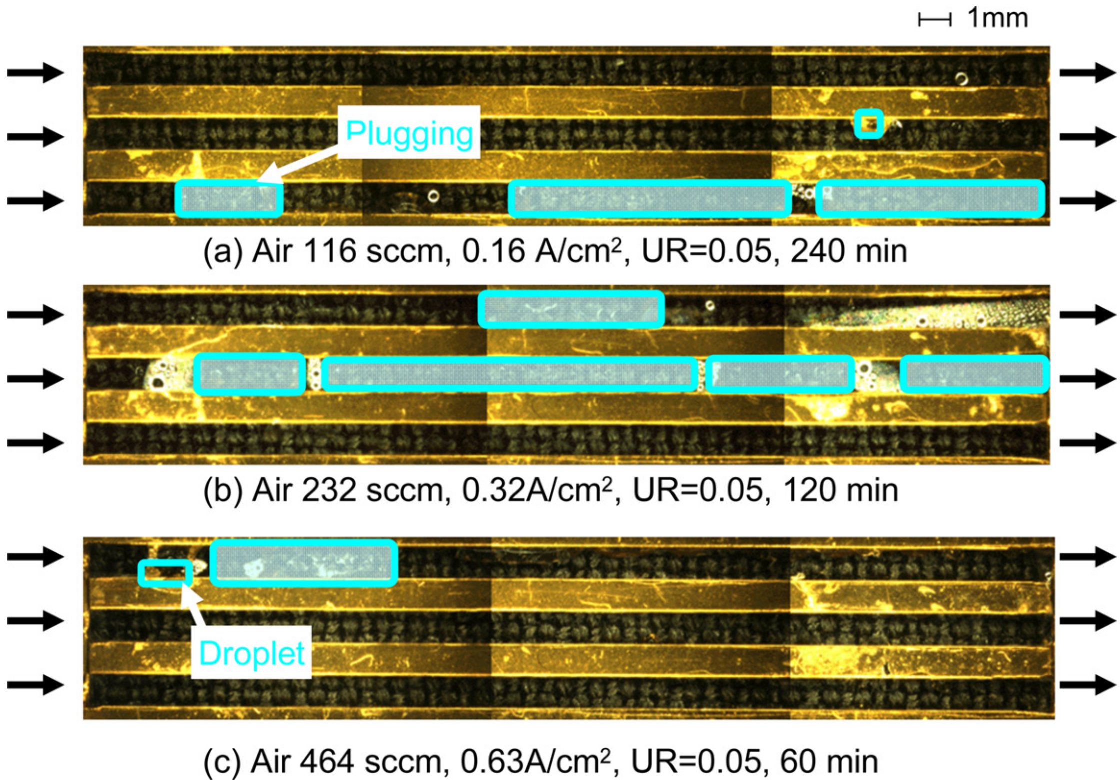

Fig. 9. Visualized images of the parallel three channels cell at the specified time under the same oxygen utilization ratio condition of 0.05.

drainage R_{dra}, which might be correspond to the drag force on water droplet, is proportional to the second power of gas velocity. Under constant utilization condition the R_{dra} becomes to be proportional to the second power of the load current. Considering these two features of R_{pro} and R_{dra}, a specific load current exists which allows the value $R_{pro} - R_{dra}$ to be maximum under the constant utilization condition. The middle current density condition of 0.3 A cm^{-2} is thought to be just the current to make the value $R_{pro} - R_{dra}$ be maximum, resulting in a most water-accumulation and unstable cell voltage.

Although we here indicated that the middle current density condition caused most water-accumulation resulting in an unstable cell voltage for both the straight one channel and parallel three channels cell, a further evaluation is advisable. There is a possibility that the instantaneous image taken at the time, as shown in Figs. 7 and 8, happened that the case of middle current density showed the maximum accumulation of droplets. To fairly confirm this statement, additional evaluation is expected, for instance, to average the amount of liquid water at each moment for long-term experiment.

Different from straight one channel and parallel three channels cells, serpentine one channel cell indicated stable cell voltage against any load-current densities as shown in Fig. 7c. In addition that the serpentine channel cell can effectively drain the water in GDL as mentioned above, faster flow velocity in channel comparing with the cases of other channel pattern cell is thought to have lead a stable cell voltage of the serpentine channel cell. Referring Table 2 along the constant oxygen utilization of 0.05, the flow velocities at the inlet of straight one channel and parallel three channels cell are 0.6, 1.2 and 2.4 m s^{-1} for 0.15, 0.3 and 0.6 A cm^{-2}, respectively. In the case of the serpentine one channel cell, they are 1.9, 3.4 and 7.7 m s^{-1}. Thus, the faster velocity is thought to have yielded the stable cell voltage of the serpentine one channel cell. In the following section, we draw a comparison between the different channel-pattern cells under a constant flow velocity at channel inlet.

3.3. Comparison under the constant inlet-flow-velocity of 1.3 m s^{-1}

Fig. 10 is cell voltage and overvoltage resistance of different channel-pattern cells under the constant inlet-flow-velocity of 1.3 m s^{-1}, with various load currents of 0.15, 0.3 and 0.6 A cm^{-2}. It is noted that the oxygen utilization ratio in the serpentine one channel cell reached three times higher than that in the other channel cells, to give the same inlet-flow-velocity condition between the cells.

The tendency of cell voltage variation for each different channel-pattern cell is again similar to Figs. 2 and 7, where we did evaluation under a constant current and oxygen-utilization condition. The straight one channel cell had monotonous decrease and sudden change. The parallel three channels and serpentine one channel cell had step-wise and saw-edge-wise change, respectively. However, even in the case of the serpentine cell a sudden large change of cell voltage was appeared when 0.6 A cm^{-2} was loaded. This is because a high oxygen utilization of 0.3 was imposed, when the current of 0.6 A cm^{-2} was loaded as shown in Table 2, leading to a large amount of water accumulation.

Although the large change was appeared, the serpentine channel cell could continue to generate electricity in spite of higher utilization ratio of 0.3 and large current density of 0.6 A cm^{-2}, which are most severer condition within this study. This superior nature of serpentine channel cell can be explained as in the following. The severe condition gives higher rate of water accumulation. But the rather high repetitive flushing events of this cell as mentioned in Section 3.1 might disturb continuous accumulation, resulting in the continuous generating. This consideration is supported by constant and low overvoltage–resistance shown in

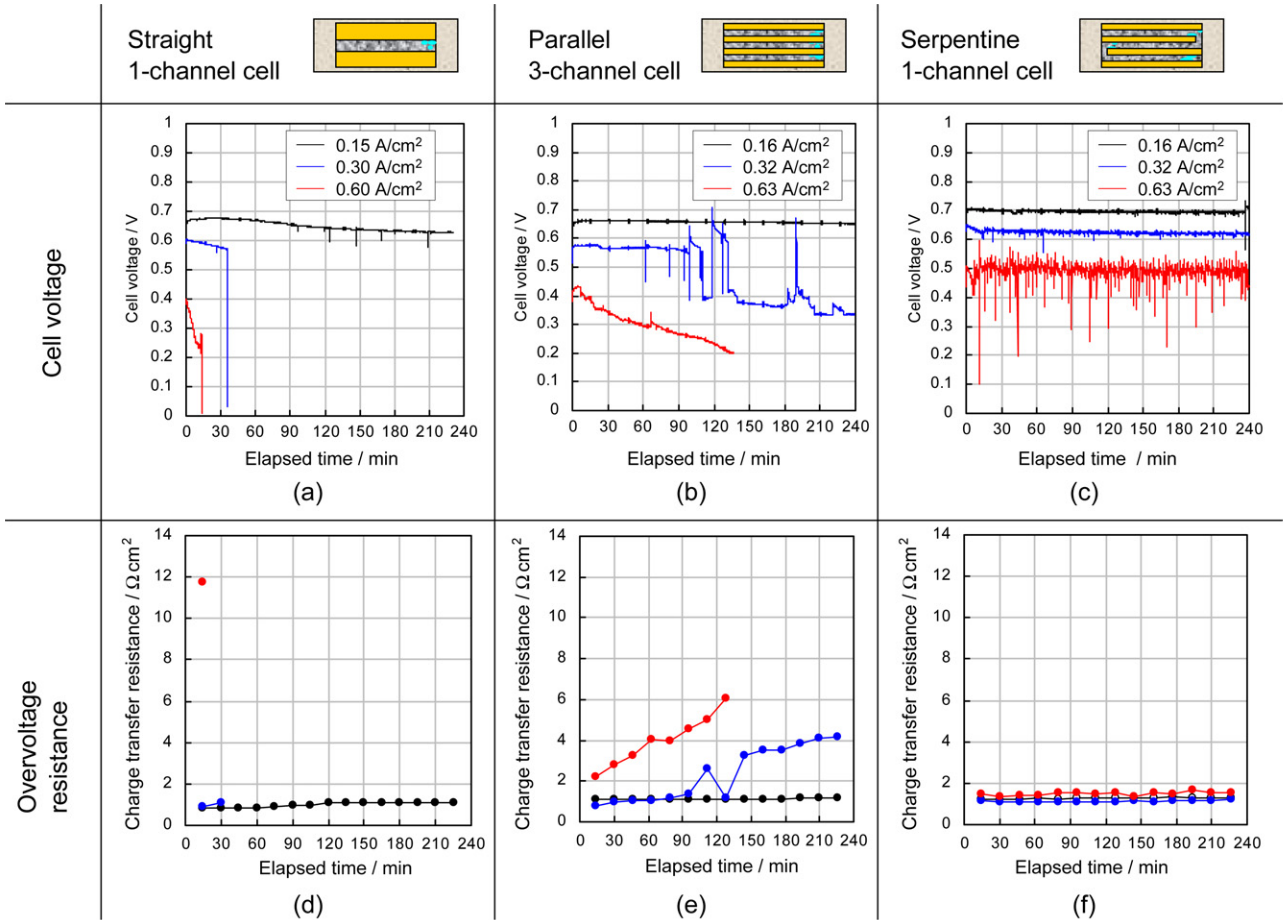

Fig. 10. Time variation of cell voltage and overvoltage resistance of the different channel-pattern cells under the same inlet-flow-velocity condition of 1.3 m s^{-1}.

Fig. 9f, which corresponds to water accumulation. Thus the serpentine one channel cell had again superior performance than the other cells even in the comparison with a constant inlet-flow-velocity.

4. Summary

For elucidating how the difference of channel pattern impacts PEFC performance and water droplet behavior in channel, we operated and visualized straight one channel, parallel three channels and serpentine one channel cell under a constant load current, oxygen utilization or inlet flow-velocity conditions. This experimental analysis gave us the followings:

(1) Cell voltage change synchronizes with the water behavior in channel. Three events of water behavior appear in turn and they repeat occasionally. First, water-accumulation monotonously reduces the voltage. Secondly, its accumulated water reaches plugging with sharply decreasing the voltage. Thirdly, plugged water is flushed with recovering the voltage. All cells pecked up in this study follow these events essentially.
(2) However each cell has an inherent water behavior, leading to a peculiar cell voltage change. The cell voltage in straight one channel cell shows monotonous decrease and sudden fluctuation. That in parallel three channels cell shows step-wise change. That in serpentine one channel cell shows saw-edge-wise change.
(3) Among the three different channel pattern cells, the serpentine one channel cell has superior performance with stable and high cell voltage, because measurable water-accumulation near the corner of channel can trigger repetitive flushing and drainage, in addition that gas flow formed under rib can promotes the drainage of water in GDL.

References

[1] Klaus Tüber, et al., J. Power Sources 124 (2003) 403.
[2] Zhang, et al., J. Electrochem. Soc. 153 (2006) A225.
[3] Xuan Liu, et al., J. Power Sources 156 (2006) 267.
[4] Xuan Liu, et al., Electrochim. Acta 52 (2007) 3607.
[5] A. Turhan, et al., J. Power Sources 160 (2006) 1195.
[6] J.J. Kowal, et al., J. Electrochem. Soc. 153 (2006) A1971.
[7] N. Pekula, et al., Nucl. Instrum. Methods Phys. Res. A 542 (2005) 134.
[8] M.V. Williams, et al., J. Electrochem. Soc. 151 (2004) A1617–1627.
[9] H. Masuda, et al., J. Power Sources 177 (2008) 303.